

Metamaterial-Based Antennas for Integration in UWB Transceivers and Portable Microwave Handsets

Mohammad Alibakhshi-Kenari,¹ Mohammad Naser-Moghadasi,¹
Ramazan Ali Sadeghzadeh,² Bal Singh Virdee³

¹Faculty of Engineering, Science and Research Branch, Islamic Azad University, Tehran, Iran

²Faculty of Electrical and Computer Engineering, K. N. Toosi University of Technology, Tehran, Iran

³London Metropolitan University, Center for Communications Technology, London, N7 8DB, United Kingdom

Received 27 May 2015; accepted 5 September 2015

ABSTRACT: Two planar antennas based on metamaterial unit-cells are designed, fabricated, and tested. The unit-cell configuration consists of H-shaped or T-shaped slits and a grounded spiral. The slits essentially behave as series left-handed capacitance and the spiral as a shunt left-handed inductance. The unit-cell was modeled and optimized using commercial 3D full-wave electromagnetic simulation tools. Both antennas employ two unit-cells, which are constructed on the Rogers RO4003 substrate with thickness of 0.8 mm and $\epsilon_r = 3.38$. The size of H-shaped and T-shaped unit cell antennas are $0.06\lambda_0 \times 0.02\lambda_0 \times 0.003\lambda_0$ and $0.05\lambda_0 \times 0.02\lambda_0 \times 0.002\lambda_0$, respectively, where λ_0 is the free-space wavelength. The measurements confirm the H-shaped and T-shaped unit-cell antennas operate across 1.2–6.7 GHz and 1.1–6.85 GHz, respectively, for voltage standing wave ratio (VSWR) < 2 , which correspond to fractional bandwidth of $\sim 140\%$ and $\sim 145\%$, respectively. The H-shaped unit-cell antenna has gain and efficiency of 2–6.8 dBi and 50–86%, respectively, over its operational range. The T-shaped unit-cell antenna exhibits gain and efficiency of 2–7.1 dBi and 48–91%, respectively. The proposed antennas have specifications applicable for integration in UWB wireless communication systems and microwave portable devices. © 2015 Wiley Periodicals, Inc. *Int J RF and Microwave CAE* 26:88–96, 2016.

Keywords: index terms; planar antennas; metamaterials; left-handed structures; ultra-wideband

I. INTRODUCTION

Portable microwave handsets are ubiquitous and have become one of the necessities of modern live. These devices have become multifunctional and provide services other than communications such as social media, internet browsing, mobile TV, and so forth. They are designed to be compact and light weight for portability, however, in their design there is a tradeoff between performance and functionalities [1–3]. The challenge in the implementation of small and compact portable devices is to incorporate

all the necessary circuitry onto a small and highly integrated wireless transceiver unit. Among all the components the antenna is one of the most challenging as its dimensions are related to the operating frequency. To eradicate this issue the use of metamaterials are becoming a very attractive solution in the design of compact planar antennas [4–7].

In this article, two miniature and compact antenna designs are described for integration in ultrawideband (UWB) wireless systems. Both antennas exhibit good overall performance in terms of radiation patterns, gain, and efficiency. The proposed antennas are based on composite right/left-handed transmission-lines (CRLH-TL) [4–6]. The metamaterial unit-cells were implemented using either an H-shaped and T-shaped slits that are embedded directly onto the radiating patch, and include a

Correspondence to: M. Naser-Moghadasi; email: mn.moghaddasi@srbiau.ac.ir.

DOI: 10.1002/mmce.20942

Published online 16 September 2015 in Wiley Online Library (wileyonlinelibrary.com).

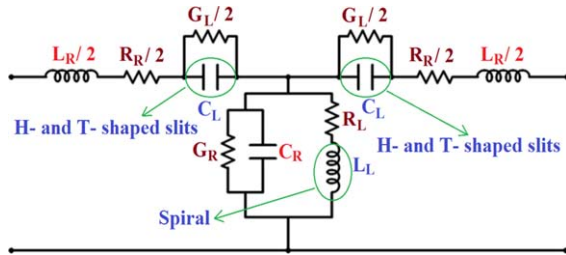


Figure 1 The equivalent circuit model of the proposed antenna.

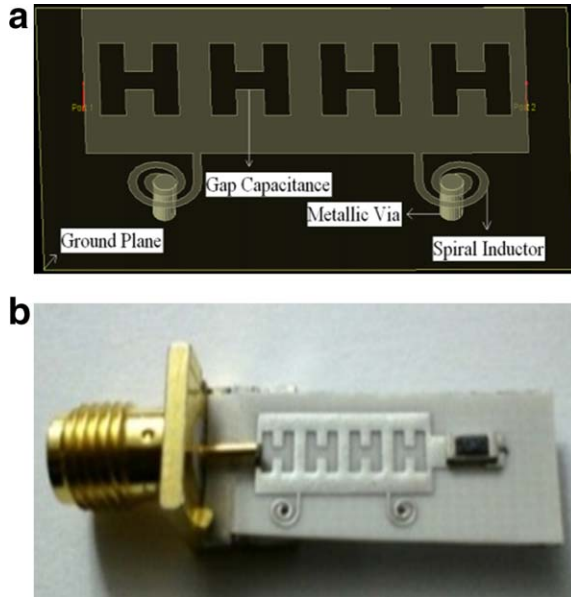


Figure 2 Antenna constructed using two H-shaped slit unit-cells.

spiral which is grounded using a via-hole. The H-shaped and T-shaped slits behave as a series left-handed capacitance, and the grounded spiral acts as a left-handed shunt inductance. Results show just two unit-cells were sufficient to realize the desired antenna performance.

II. DESIGN OF THE PROPOSED ANTENNAS

A. H-Shaped Slit Antenna

The equivalent circuit model of the H-shaped slit antenna is based on the composite right/left-handed transmission-line structure shown in Figure 1. Standard printed circuit board manufacturing techniques were employed in the

TABLE I H-Shaped Slit Antenna Parameters

Length of H-slits (L_H)	3.0 mm
Width of H-slits (W_H)	0.7 mm
Distance between slits (D_H)	0.7 mm
Width of spirals (W_S)	0.2 mm
Spacing of spirals (S_S)	0.2 mm
Number of spirals turns (N)	2
Height of via-hole (h)	0.8 mm
Length of 50-Ω load (SMD1206)	4.2 mm

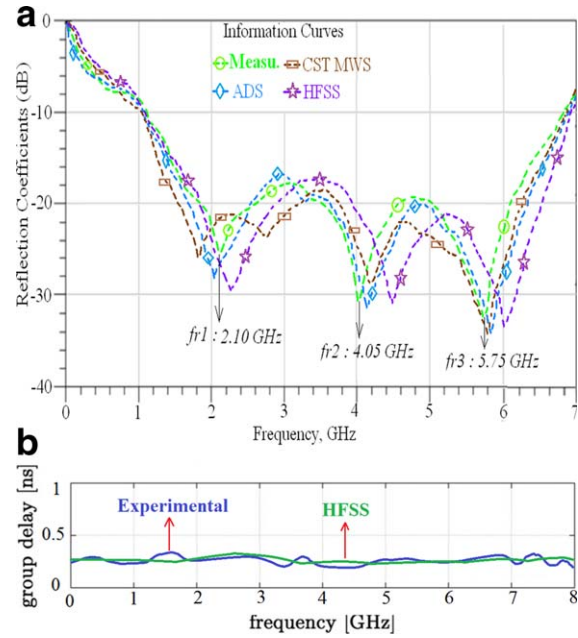


Figure 3 (a) Simulated and measured reflection-coefficient response of the H-shaped slit antenna, and (b) group-delay of the H-shaped slit antenna.

implementation of series left-handed capacitors (C_L) and the shunt left-handed inductors (L_L). The H-shaped slits and the spiral inductors were etched directly on the radiation patch. Each unit-cell is composed of two H-shaped slits with an inductive spiral placed between the slits. The spiral is connected to the ground-plane through a metallic via-hole. The proposed technique significantly reduces the physical foot print of UWB antennas because unlike conventional antennas it is independent of wavelength. The parasitic series right-handed inductance (L_R) and shunt right-handed capacitance (C_R) are generated in the structure due to current flow in the metallization resulting in voltage gradients between the metal patterns of the trace and the ground-plane. As the magnitudes of these parameters are negligible. The proposed antenna was designed and fabricated on Rogers RO4003 substrate with dielectric constant of 3.38 and 0.8 mm thickness. Figure 2 shows

TABLE II H-Shaped Slit Antenna Characteristics

Dimensions	Electrical: $0.06 \lambda_0 \times 0.02 \lambda_0 \times 0.003 \lambda_0$ at 1.2 GHz Physical: $15 \times 6.9 \times 0.8 \text{ mm}^3$
Bandwidth (BW)	Measured: 1.2–6.7 GHz, fractional BW = 139% ADS: 1.1–6.8 GHz, fractional BW = 144% CST MWS: 1.05–6.75 GHz, fractional BW = 146% HFSS: 1.15–6.82 GHz, fractional BW = 142%
Gain (dBi)	2, 2.5, 6.8, 5.4, and 4.3
Efficiency (%)	50, 55, 86, 72, and 65

Gain and efficiency measured at 1.2, 2.1, 4.05, 5.75, and 6.7 GHz

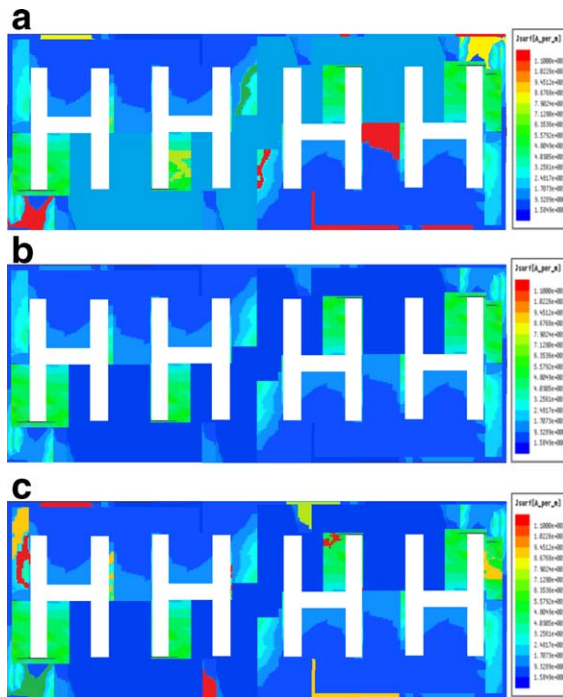


Figure 4 Current distribution over the H-shaped slit antenna structure at various resonance frequencies.

the configuration of the antenna, which consists of two metamaterial unit-cells embedded in the radiating patch. Each unit-cell is composed of two H-shaped slits with an inductive spiral which is grounded through a metallic via-hole. The antenna is excited from left-hand side through a 50- Ω microstrip feed-line. The right-hand side of the patch is terminated with a matched load of 50 Ω .

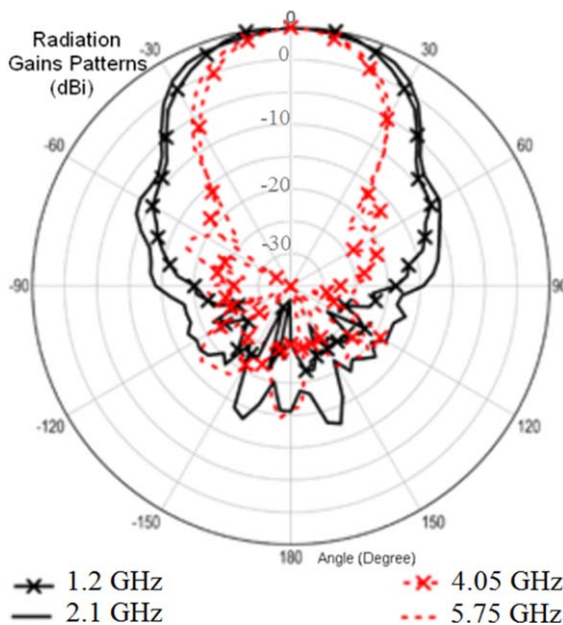


Figure 5 Measured radiation patterns of the H-shaped slit antenna.

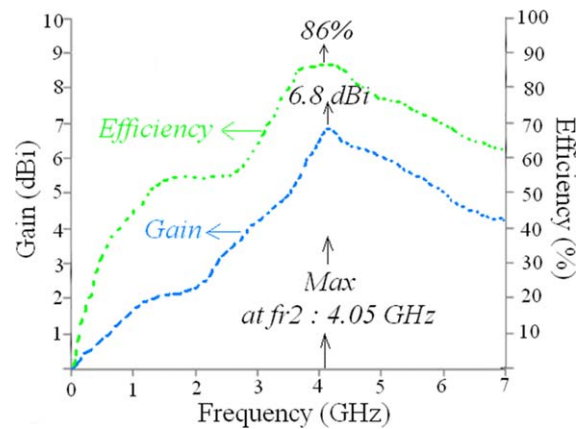


Figure 6 Measured gain and efficiency response of the H-shaped slit antenna.

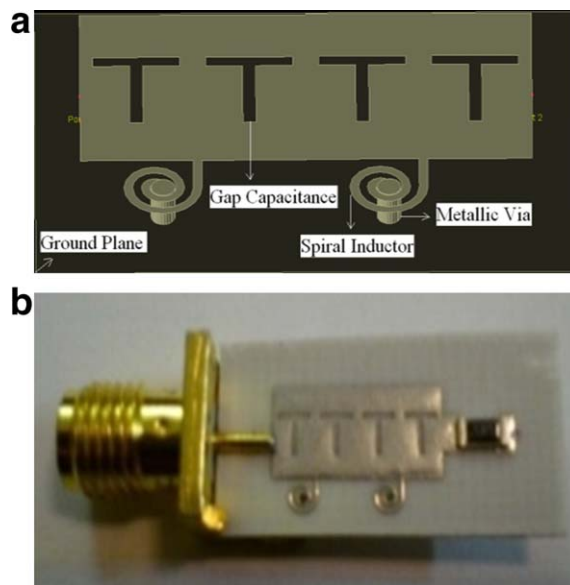


Figure 7 Antenna using two T-shaped slit unit-cells.

(SMD1206) that is connected to ground-plane through a metallic via-hole. In the structure the unit-cells occupy a surface area of $5.4 \times 6.9 \text{ mm}^2$ or $0.02\lambda_0 \times 0.02\lambda_0$, where λ_0 is the free-space wavelength at 1.2 GHz. The total electrical length, width and height of antenna are $0.06\lambda_0$, $0.02\lambda_0$, and $0.003\lambda_0$, which correspond to 15 mm, 6.9 mm, and 0.8 mm, respectively.

TABLE III T-Shaped Slit Antenna Parameters

Length of T-slits	3.0 mm
Width of T-slits	0.4 mm
Distance between slits	0.4 mm
Width of spirals	0.2 mm
Spacing of spirals	0.2 mm
Turns of spirals	2
Height of via-hole	0.8 mm
Length of 50- Ω load (SMD1206)	4.2 mm

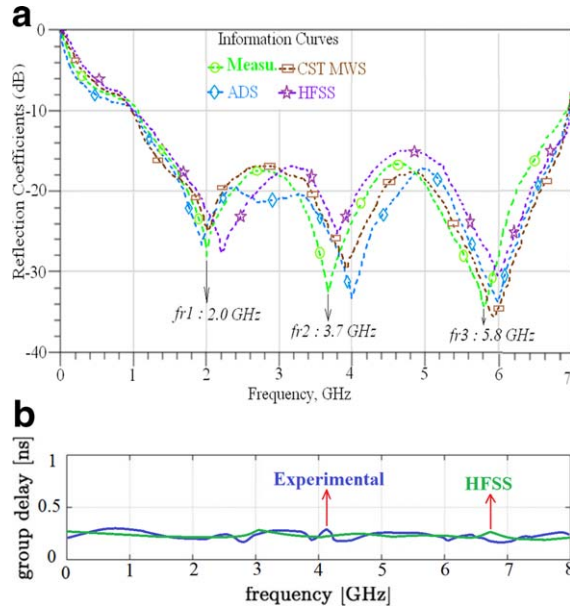


Figure 8 (a) Simulated and measured reflection-coefficient response of the T-shaped slit antenna, and (b) group-delay of the T-shaped slit antenna.

Besides the compactness and small size, the other performance parameters of antenna that need to be met were UWB bandwidth and radiation properties. As will be shown later the two aforementioned parameters can be realized by appropriately selecting the number of metamaterial unit-cells. The unit-cell which is constructed from a pair of slits and spiral were optimized using 3D full-wave electromagnetic simulators, that is, Agilent Advanced Design System (ADS), High Frequency Structure Simulator (HFSS) and CST Microwave Studio (CST MWS). Optimization involved tradeoff between antenna bandwidth, gain, and efficiency performance. The optimized parameters of the antenna in Figure 1 are given in Table I.

The fabricated antenna's performance was measured using a standard antenna set-up. The measured reflection-coefficient response of the antenna is shown in Figure 3a. The antenna operates between 1.2 and 6.7 GHz for volt-

TABLE IV T-Shaped Slit Antenna Characteristics

Dimensions	Electrical: $0.05\lambda_0 \times 0.02\lambda_0 \times 0.002\lambda_0$ at 1.1 GHz Physical: $15.5 \times 6.9 \times 0.8 \text{ mm}^3$
Bandwidth (BW)	Measured: 1.1–6.85 GHz, fractional BW = 144% ADS: 1.05–6.9 GHz, fractional BW = 147% CST MWS: 1–6.88 GHz, fractional BW = 149% HFSS: 1–6.95 GHz, fractional BW = 149%
Gain (dBi)	2, 2.7, 7.1, 5.9, and 5
Efficiency (%)	48, 60, 91, 88, and 73
Gain and efficiency measured at 1.1, 2, 3.7, 5.8, and 6.85 GHz	

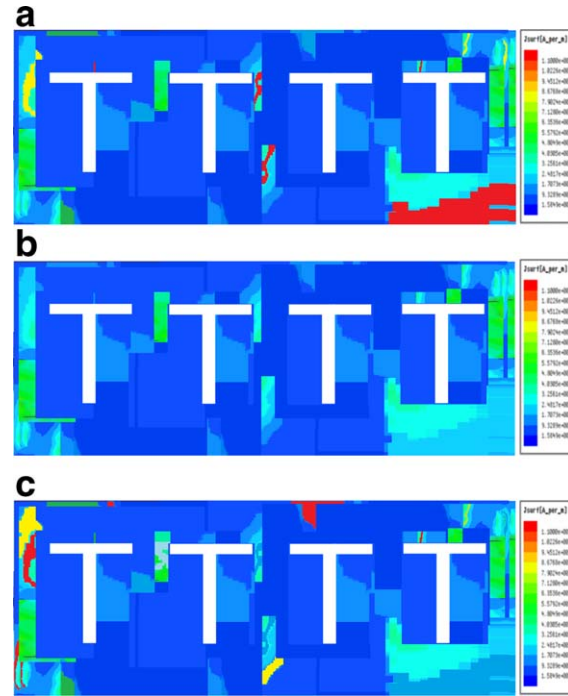


Figure 9 Current distributions over the T-shaped slit antenna structure at various resonance frequencies.

age standing wave ratio (VSWR) < 2 , which corresponds to a fractional bandwidth of 139%. In this range, the antenna resonates at three distinct frequencies, that is, 2.1, 4.05, and 5.75 GHz. The maximum gain and efficiency are measured at 4.05 GHz, that is, 6.8 dBi and 86%, respectively. The simulated and measured group-delay of the antenna in Figure 3b shows is about 0.25 ns across

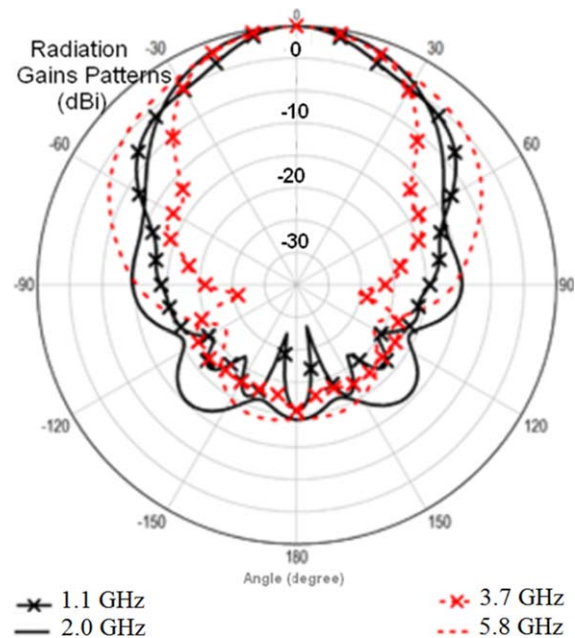


Figure 10 Measured radiation patterns of the T-shaped slit antenna.

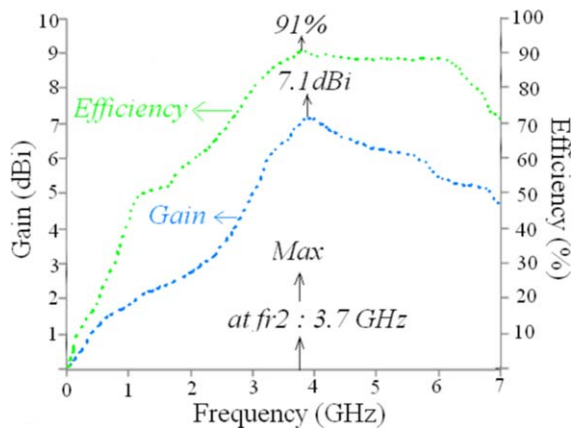


Figure 11 Measured gain and efficiency response of the T-shaped slit antenna.

0–8 GHz. The characteristics of the H-shaped antenna are listed in Table II.

The current density distributions over the antenna structure at the three resonant frequencies are shown in Figure 4. The radiation patterns of the antenna at the resonant frequencies in Figure 5 shows that the antenna is directional, and at higher frequencies (4.05 and 5.75 GHz) its 3 dB beamwidth reduces by approximately 30%. The measured gain and efficiency response, shown in Figure 6, reveal the antenna can operate between 0 and 7 GHz, with a peak gain and efficiency of 6.8 dBi and 86% at 4.05 GHz.

B. T-Shaped Slit Antenna

A variation to the previous H-shaped printed antenna is presented here which is constituted from two metamaterial unit-cells consisting of T-shaped slits that are embedded in the radiating patch with inductive spiral terminated to the ground-plane using a metallic via-hole. The configuration of the T-shaped antenna is shown in Figure 7. As

with the H-shaped antenna, the T-shaped antenna is excited through a 50-Ω feed-line connected on the left-hand side of the antenna. The antenna is terminated on the right-hand side with a matched load of 50 Ω (SMD1206). The T-shaped antenna was also fabricated on Rogers RO4003 substrate with dielectric constant of $\epsilon_r = 3.38$ and thickness of 0.8 mm. The design process of this antenna is identical to the H-shaped antenna. Each unit-cell occupies an area of $5.65 \times 6.9 \text{ mm}^2$ or $0.02\lambda_0 \times 0.02\lambda_0$, where λ_0 is free-space wavelength at the operating frequency of 1.1 GHz. The overall physical size of the T-shaped antenna is $15.5 \times 6.9 \times 0.8 \text{ mm}^3$ or $0.05\lambda_0 \times 0.02\lambda_0 \times 0.002\lambda_0$. The design parameters of the antenna are given in Table III. For the optimized parameters in Table III, the equivalent circuit parameters C_L , L_L , C_R , and L_R are 5 pF, 6.4 nH, 1 pF, and 2.8 nH, respectively.

The measured bandwidth of the T-shaped antenna extends from 1.1 to 6.85 GHz for VSWR < 2, which corresponds to a fractional bandwidth of 144%. The antenna resonates at three frequencies, that is, 2, 3.7, and 5.8 GHz, as shown in Figure 8a. The measured gain and efficiency of antenna have a maximum value of 7.1 dBi and 91%, respectively, at 3.7 GHz. The simulated and measured group-delay of the antenna is shown in Figure 8b. The average group-delay is about 0.25 ns across 0–8 GHz. The characteristics of the T-shaped antenna are listed in Table IV.

The current distribution over the T-shaped slit antenna structure at spot frequencies of 2, 3.7, and 5.8 GHz are shown in Figure 9. The measured radiation patterns at three spot frequencies in Figure 10 show the antenna radiates directionally. The measured gain and efficiency response of the antenna in Figure 11 shows the antenna operates from 0 to 7 GHz with a maximum gain and efficiency of 7.1 dBi and 91%, respectively, at 3.7 GHz.

The above results show the T-shaped slit antenna exhibits a better performance in terms of bandwidth, gain and efficiency compared to the H-shaped slit antenna.

TABLE V Comparison of the Proposed Antennas

Ref.	Dimensions	Factional Bandwidth (%)	Max. Gain (dBi)	Max. Eff. (%)
[6]-a	$0.45\lambda_0 \times 0.17\lambda_0 \times 0.02\lambda_0$	74	2.1	44
[6]-b	$0.42\lambda_0 \times 0.17\lambda_0 \times 0.041\lambda_0$	83	3.11	59
[8]-a	$0.04\lambda_0 \times 0.021\lambda_0 \times 0.002\lambda_0$	105	2.3	62
[8]-b	$0.05\lambda_0 \times 0.01\lambda_0 \times 0.002\lambda_0$	124	2.8	70
[9]	$0.44\lambda_0 \times 0.22\lambda_0 \times 0.008\lambda_0$	18	2.2	17
[10]	$0.24\lambda_0 \times 0.3\lambda_0 \times 0.009\lambda_0$	8	1.5	58
H-slit ant.	$0.06\lambda_0 \times 0.02\lambda_0 \times 0.003\lambda_0$	139	6.8	86
T-slit ant.	$0.05\lambda_0 \times 0.02\lambda_0 \times 0.002\lambda_0$	144	7.1	91

TABLE VI Equivalent Circuit Antenna Parameters

H-Shape Slit Antenna							
C_L	L_L	C_R	L_R	R_L	G_L	R_R	G_R
5.8 pF	6.4 nH	0.9 pF	2.7 nH	1.7 Ω	1.45 S	1.1 Ω	0.95 S
T-Shape Slit Antenna							
C_L	L_L	C_R	L_R	R_L	G_L	R_R	G_R
5 pF	6.4 nH	1 pF	2.8 nH	1.85Ω	1.5 S	1.05Ω	0.8 S

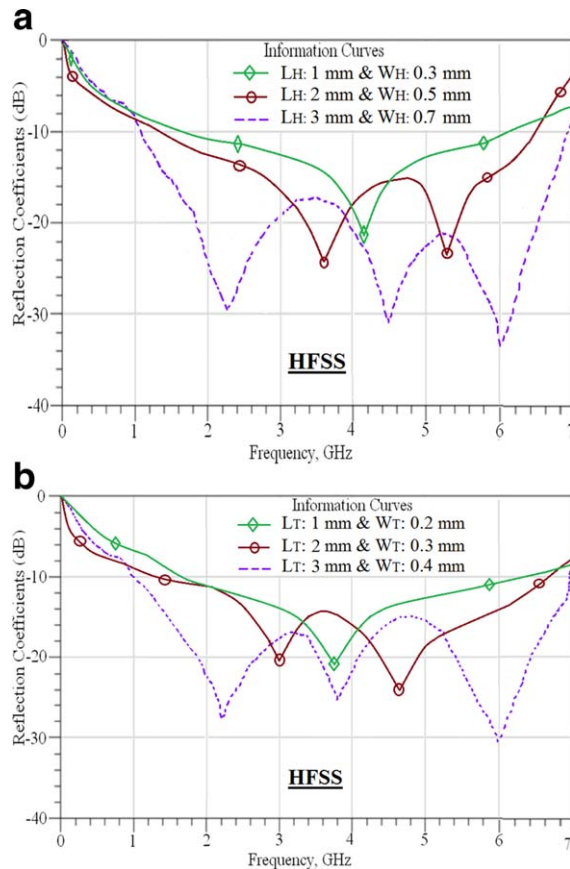


Figure 12 Effect of slit length and width on the antenna bandwidth.

Comparison of the proposed antennas with other conventional antennas in terms of size, gain and efficiency performance are given in Table V. It is evident the proposed H-shaped and T-shaped antennas offer superior performance.

For the optimized antenna parameters in Tables I and III, the corresponding equivalent circuit parameters representing the left-handed and right-handed variables C_L , L_L , C_R , L_R , R_L , G_L , R_R , and G_R are listed in Table VI. This table shows the equivalent capacitive and inductive parameters of both the T-shaped and H-shaped slit antennas. The parameters of both the T-shaped and H-shaped slit antennas are virtually identical except for the left-handed capacitance (C_L), which has a bearing on its performance. Moreover, the T-shape antenna is significantly smaller than the H-shaped antenna by 44.4%.

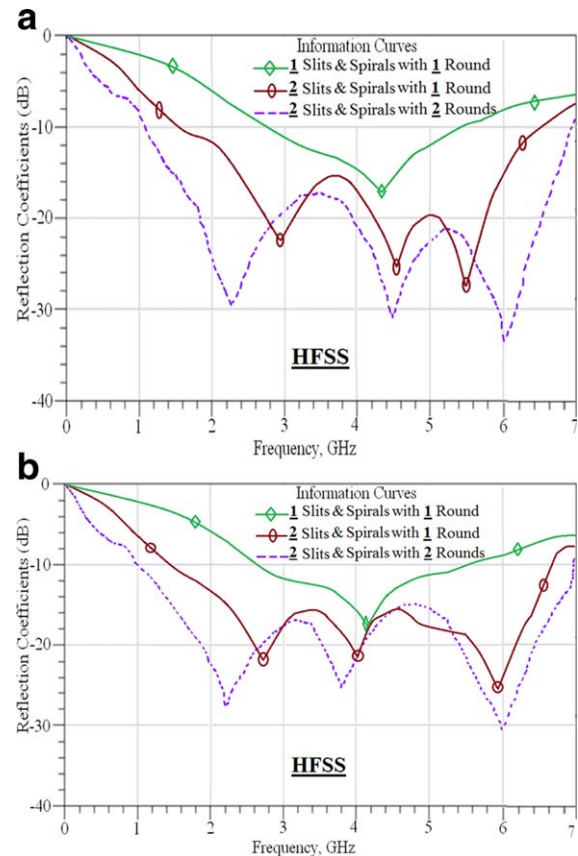


Figure 13 Bandwidths responses as a function number of slits in each of unit cells accompanying the number of spiral rounds.

III. PARAMETRIC STUDY

The effect of the slit dimensions on the antenna characteristics was investigated. It is evident from Figure 12 that by increasing in the length and width of the slits improves the antenna's impedance bandwidth and matching performance. The results are given in Table VII. By increasing the length and width of the H-shaped slit antenna from 1 mm and 0.3 mm to 3 mm and 0.7 mm, respectively, improves its fractional bandwidth from 116 to 142%. In the case of the T-shaped slit antenna, the bandwidth improves by 25% from 119 to 149% for increase in slit length from 1 to 3 mm, and width from 0.2 to 0.4 mm.

TABLE VII Bandwidth Response as a Function of Antenna Length and Width

	Bandwidth (GHz)	Fractional Bandwidth	No. of Resonances	S_{11} (dB)
H-Shape Slit Antenna				
$L_H = 1$ mm & $W_H = 0.3$ mm	1.62–6.1	116%	One	< -20
$L_H = 2$ mm & $W_H = 0.5$ mm	1.35–6.45	130%	Two	< -25
$L_H = 3$ mm & $W_H = 0.7$ mm	1.15–6.82	142%	Three	< -30
T-Shape Slit Antenna				
$L_T = 1$ mm & $W_T = 0.2$ mm	1.6–6.35	119%	One	< -20
$L_T = 2$ mm & $W_T = 0.3$ mm	1.3–6.65	134%	Two	< -25
$L_T = 3$ mm & $W_T = 0.4$ mm	1.0–6.95	149%	Three	< -30

TABLE VIII Bandwidth Response as a Function Number of Slits and Spiral Turns in Each Unit-Cell

	Bandwidth (GHz)	Fractional Bandwidth	No. of Resonances	S_{11} (dB)
H-Shape Slit Antenna				
1 slit & 1 spiral turn	2.75–5.42	65%	One	< -20
2 slits & 1 spiral turn	1.55–6.45	122%	three	< -25
2 slits & 2 spiral turns	1.15–6.82	142%	three	< -30
T-Shape Slit Antenna				
1 slit & 1 spiral turn	2.65–5.55	70%	One	< -20
2 slits & 1 spiral turn	1.45–6.62	128%	three	< -25
2 slits & 2 spiral turns	1.0–6.95	149%	three	< -30

The number of slits and number of spiral round turns were also investigated. By increasing the number slits in each unit-cell and number of spiral round turns also had a positive impact on the antenna's bandwidth and match properties, as shown in Figure 13. It is observed that by increasing the number of slits causes the number of resonance frequencies to increase too. The summarized results in Table VIII indicate that by increasing the number of slits from 1 to 2, the fractional bandwidth of both antennas increases by approximately twofolds.

The gain and radiation efficiency of the antennas as a function of slit dimensions, the number of slits in the

unit-cell and number of spiral round turns were also investigated. It is evident that by increasing the length and width of slits, in Figures 14a and 14b, and increasing the number of slits and number of spiral round turns, in Figures 14c and 14d, the gain and radiation efficiency increase considerably. This is attributed to increase in the antenna aperture.

IV. CONCLUSIONS

The design and implementation of miniature UWB antennas using metamaterial unit-cells was described. The

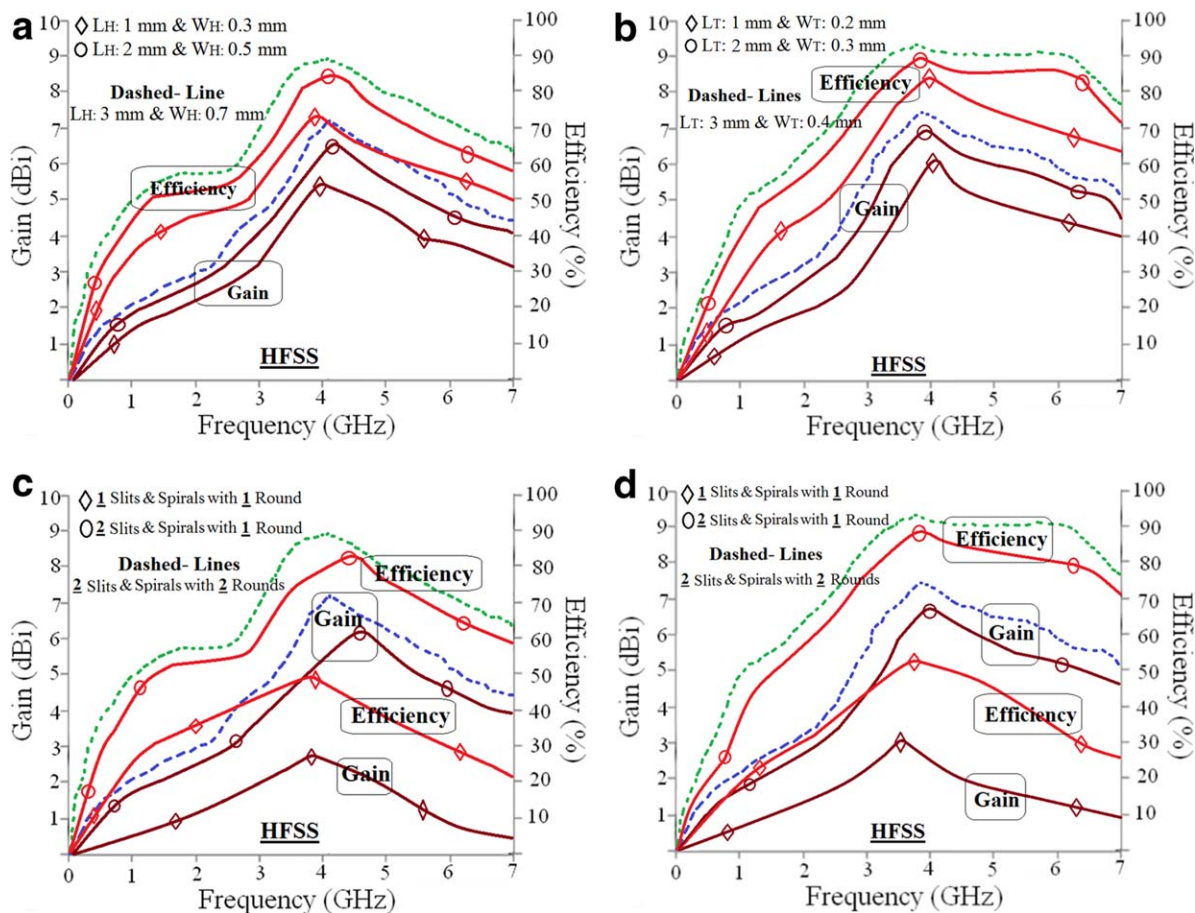


Figure 14 (a) and (b) Gain and radiation efficiency as a function of slit dimensions and (c) and (d) number of slits and number of spiral turns.

metamaterial unit-cell was composed of H-shaped or T-shaped slits embedded in the radiating patch with a grounded inductive spiral using a metallic via-hole. The slits essentially act as left-handed capacitance and the spiral left-handed inductance. The performance of the antennas was optimized and verified practically. The H-shaped antenna operated over 1.2–6.7 GHz (fractional bandwidth $\sim 140\%$) with a maximum gain and efficiency of 6.8 dBi and 86% at 4.05 GHz. The electrical size of the antenna is $0.06\lambda_0 \times 0.02\lambda_0 \times 0.003\lambda_0$. The T-shaped antenna operates over 1.1–6.85 GHz (fractional bandwidth $\sim 145\%$) with a maximum gain and efficiency of 7.1 dBi and 91% at 3.7 GHz. This antenna has an electrical size of $0.05\lambda_0 \times 0.02\lambda_0 \times 0.002\lambda_0$. Both antennas exhibit superior performance compared to conventional antennas in terms of fractional bandwidth, gain and efficiency. The antennas are suitable for UWB wireless communication systems, portable microwave handsets, and transceivers.

REFERENCES

1. C. Picher, J. Anguera, A. Andújar, C. Puente, and S. Kahng, Analysis of the human head interaction in handset antennas with slotted ground planes, *IEEE Antennas Propag Mag* 54 (2012), 36–56.
2. J. Anguera, A. Andújar, M.-C. Huynh, C. Orlenius, C. Picher, and C. Puente, Advances in antenna technology for wireless handheld devices, Article ID: 838364, *Int J Antennas Propag* 2013 (2013), 1–25.
3. A. Al-Rawi, A. Hussain, J. Yang, M. Franzén, C. Orlenius, and A.A. Kishk, A new compact wideband MIMO antenna—the double-sided tapered self-grounded monopole array, *IEEE Trans Antennas Propag* 62 (2014), 3365–3369.
4. M. Alibakhshi-Kenari, M. Naser-Moghadasi, R.A. Sadeghzadah, Bandwidth and radiation specifications enhancement of monopole antennas loaded with split ring resonators, *IET Microwave Antennas Propag*, 10 pp, DOI: 10.1049/iet-map.2015.0172. Online ISSN 1751-8733. Available online: 23 July 2015.
5. M. Alibakhshi-Kenari, M. Naser-Moghadasi, and R.A. Sadeghzadah, The resonating MTM based miniaturized antennas for wide-band RF-microwave systems, *Microwave Opt Technol Lett* 57 (2015), 2339–2344.
6. M. Alibakhshi-Kenari, Introducing the new wideband small plate antennas with engraved voids to form new geometries based on CRLH MTM-TLs for wireless applications, *Int J Microwave Wireless Technol* 6 (2014), 629–637.
7. X. Mi Yang, Q. Hui Sun, Y. Jing, Q. Cheng, X. Yang Zhou, H. Wei Kong, and T. Jun Cui, Increasing the bandwidth of microstrip patch antenna by loading compact artificial magnetodielectrics, *IEEE Trans Antennas Propag* 59 (2011), 373–378.
8. M. Alibakhshi-Kenari, Printed planar patch antennas based on metamaterial, *Int J Electronic Lett* 2 (2014), 37–42.
9. C.J. Lee, M. Achour, and A. Gummalla, Compact metamaterial high isolation MIMO antenna subsystem, In: *Asia-Pacific Microwave Conference*, Macau, 2008, pp. 1–4.
10. C.-C. Yu, M.-H. Huang, L.-K. Lin, Y.-T. Chang, A compact antenna based on metamaterial for WiMAX, In: *Asia-Pacific Microwave Conference*, Macau, 2008, pp. 1–4.

BIOGRAPHIES



Mohammad Alibakhshi-Kenari was born in Freydonkenar, Iran on February 1988. He received the B.Sc. and M.Sc. degrees both in the Electrical Engineering, field of Telecommunication from the Islamic Azad University, Najafabad Branch of Esfahan-Iran on February 2010 and the Islamic Republic of Iran, Shahid Bahonar university of Kerman on February 2013, respectively. His researches interests include microwave and millimeter-wave circuits, transceivers, antennas and wave-propagation, CRLH-TLs, metamaterials, Integrated RF-technologies, embedded systems, electromagnetic-waves applications, and wireless telecommunication systems. He is now “Editor-in-Chief” in Journal Club for Electronic and Communication Engineering and member of the Applied Computational Electromagnetics Society (ACES), so too works as a reviewer in the several good journals such as IEEE TIE, IET MAP, OSA, Wiley, Elsevier, Taylor & Francis, Springer and ACES Journals and so forth. Mr. M. Alibakhshi-Kenari has too served as a M-TPC of some of the international conferences. So far, he has been published several journal papers.



Mohammad Naser-Moghadasi was born in Iran, in 1959. He received the B.Sc. degree in Communication Eng. in 1985 from the Leeds Metropolitan University (formerly Leeds Polytechnic)-UK. Between 1985 and 1987, he worked as an RF-design-engineer for the Gigatech company in Newcastle Upon Tyne-UK. From 1987 to 1989, he was awarded a full schol-

arship by the Leeds Educational Authority to pursue an M.Phil. on Studying CAD of microwave-circuits. He received his Ph.D. in 1993, from the University of Bradford-UK. He was offered then a 2-years post-doc. at the University of Nottingham-UK, to pursue research on microwave cooking of materials. From 1995, Dr. Naser-Moghadasi joined Islamic Azad University, Science and Research Branch, Iran-Tehran, where he currently is head of post-graduate studies. His main areas of interest in research are microstrip antenna, microwave passive and active circuits, RF MEMS. Dr. Naser-Moghadasi is member of the IET, MIET and IEICE. He has so far published over 150 papers.



Ramazan Ali Sadeghzadeh received his B.Sc. in 1984 in Telecommunication Engineering from the Khajeh Nassir Toosi, University of Technology, Tehran-Iran, and M.Sc. in digital Communications Engineering from the University of Bradford and UMIST (University of Manchester, Institute of Science and Technology)-UK, as a joint program in 1987. He received his Ph.D. in electromagnetic and antenna from the University of Bradford-UK, in 1990. He worked as a Post-Doctoral Research assistant in the field of propagation, electromagnetic, antenna, Bio-Medical, and Wireless communications from 1990 till 1997. From 1984 to 1985 he was with Telecommunication Company of Iran (TCI) working on Networking. Since 1997 he is with K.N. Toosi University of Technology working with Telecommunications Dept. at faculty of Electrical and Computer Engineering. He has published more than 75 referable papers in international journals and conferences. Dr. Sadeghzadeh’s current interests are numerical techniques in electromagnetic, antenna, propagation, radio networks, wireless communications, nanoantennas, and radar-systems.



Bal Singh Virdee received the B.Sc. and MPhil degrees in Communications-Engineering from the University of Leeds-UK and his Ph.D. in Electronic-Engineering from the University of London-UK. He has worked in industry for various companies including Philips (UK) as an R&D-engineer and Filtronic-Components Ltd. as a future products developer in the area of RF/microwave communications. He has taught at several academic institutions before joining London Met-

ropolitan University where he is a Professor of Microwave-Communications in the Faculty of Life Sciences & Computing where he Heads the Center for Communications-Technology and is the Director of London Metropolitan-Microwaves. His research, in collaboration with industry and academia, is in the area of microwave wireless communications encompassing mobile-phones to satellite-technology. Prof. Virdee has chaired technical sessions at IEEE international conferences and published numerous research-papers. He is Executive-Member of IET's Technical and Professional Network Committee on RF/Microwave-Technology. He is a Fellow of IET and a Senior-Member of IEEE.